

## Synthesis and Evaluation of $^{18}\text{F}$ -Labeled 2-Phenylbenzothiazoles as Positron Emission Tomography Imaging Agents for Amyloid Plaques in Alzheimer's Disease

Kim Serdons,\*<sup>†</sup> Christelle Terwinghe,<sup>‡</sup> Peter Vermaelen,<sup>‡</sup> Koen Van Laere,<sup>‡</sup> Hank Kung,<sup>§</sup> Luc Mortelmans,<sup>‡</sup> Guy Bormans,<sup>†</sup> and Alfons Verbruggen<sup>†</sup>

Laboratory for Radiopharmacy, Faculty of Pharmaceutical Sciences, Katholieke Universiteit Leuven, Leuven, Belgium, Department of Nuclear Medicine, U. Z. Gasthuisberg, Leuven, Belgium, and Department of Radiology, University of Pennsylvania, Philadelphia

Received October 23, 2008

Imaging agents targeting amyloid  $\beta$  ( $A\beta$ ) may be useful for early diagnosis and follow-up of treatment of patients with Alzheimer's disease (AD). Three of five tested 2-(4'-fluorophenyl)-1,3-benzothiazoles displayed high binding affinities for  $A\beta$  plaques in AD human brain homogenates ( $K_i$  between 2.2 and 22.5 nM). They all contained the  $^{18}\text{F}$ -label directly attached to the aromatic ring and were synthesized starting from the nitro precursor. Determination of the partition coefficient, biodistribution studies in normal mice, and in vivo  $\mu\text{PET}$  studies in normal rats showed that their initial brain uptake was high and brain washout was fast. The most promising compound [ $^{18}\text{F}$ ]5, or 6-methyl-2-(4'-[ $^{18}\text{F}$ ]fluorophenyl)-1,3-benzothiazole, seemed to be metabolically stable in the brain, and its plasma radiometabolites, which do not cross the blood–brain barrier, were determined. The preliminary results strongly suggest that this new fluorinated compound is a promising candidate as an  $A\beta$  plaque imaging agent for the study of patients with AD.

### Introduction

Alzheimer's disease (AD<sup>6</sup>) is a progressive and fatal neurodegenerative brain disorder associated with progressive memory loss and decrease of cognitive functions, which may be accompanied by behavioral symptoms including agitation, anxiety, depression, or psychosis. It is the most common form of dementia affecting millions of elderly people. Neurohistopathologically, AD is characterized by the presence of extracellular depositions of amyloid  $\beta$  ( $A\beta$ ), intracellular neurofibrillary tangles (NFTs), activated microglia, and reactive astrocytes.<sup>1</sup> This triade of amyloid plaques, neurofibrillary tangles, and dementia was first described by Alois Alzheimer in 1907.<sup>2</sup>

The presence of amyloid plaques seems to play a major role in the AD pathogenesis.<sup>3</sup> Early detection and quantification of these hallmarks in brain with noninvasive techniques such as positron emission tomography (PET) would allow presymptomatic identification of patients and monitoring the effectiveness of novel treatments.

Clinical diagnosis of AD is now done by neuropsychological tests (Mini-Mental State Examination), but this only yields indirect information. Immunohistochemical fluorescent staining of brain tissue with highly conjugated dyes (Congo red,

chrysin G, thioflavin S, or thioflavin T), amyloid  $\beta$  antibodies, or a modified Bielschowsky technique (silver stain) can give direct information but only post mortem.<sup>4</sup> Although these highly conjugated fluorescent molecules display desirable properties, such as high binding affinity and moderate lipophilicity, their charge and large structure prevent them from crossing the intact blood–brain barrier (BBB). To allow noninvasive in vivo imaging and diagnosis of AD in an early-to-moderate stage and monitoring of the progression and effectiveness of treatment, the search for a clinically useful radiolabeled derivative of one of these dyes has become subject of worldwide research.

In the past years, radiolabeled derivatives of a number of the higher mentioned dyes have been tested and reported (Figure 1). X-34 derivatives consisting of only half the X-34 molecule without carboxylic groups, the so-called stilbenes (SBs), showed promising results.<sup>5</sup> The recently reported carbon-11 labeled SB-13 has already been tested in subjects with mild to moderate AD and healthy controls, showing a high accumulation in the frontal and temporoparietal cortex of patients with AD but not in age-matched control subjects.<sup>6</sup> Barrio and co-workers, on the other hand, developed [ $^{18}\text{F}$ ]FDDNP, a naphthalene derivative that binds to amyloid  $\beta$  at a different binding site and also to the NFTs.<sup>7</sup> This compound has been tested in subjects with AD, mild cognitive impairment (MCI, which may progress to AD), and no cognitive dysfunction. Small et al. reported a significantly higher binding in subjects with AD than in those with MCI or control subjects and higher binding in MCI patients than in control subjects, indicating the potential usefulness of this compound for early diagnosis of AD.<sup>8</sup> The most promising of the reported compounds are uncharged derivatives of thioflavin-T such as [ $^{125}\text{I}$ ]TZDM<sup>9</sup> and the carbon-11 labeled 2-phenylbenzothiazoles BTA and 6-OH-BTA, also known as Pittsburgh compound-B (PIB).<sup>10</sup> Of these two, PIB has the most favorable pharmacokinetics and has already been tested intensively in several clinical studies showing clear differences between AD, MCI, and control subjects.<sup>11,12</sup> Other reported compounds with high affinity for amyloid  $\beta$  are iodine-123 and fluorine-18 labeled IBOX<sup>13</sup> and IMPY,<sup>14</sup> fluorine-18 labeled acridine orange analogue BF-108,<sup>15</sup> and the recently reported fluorine-18 labeled

\* To whom correspondence should be addressed. Address: Herestraat 49 bus 821 BE, 3000 Leuven, Belgium. Phone: +32 16 330441. Fax: +32 16 330449. E-mail: kim.serdons@pharm.kuleuven.be.

<sup>†</sup> Laboratory for Radiopharmacy.

<sup>‡</sup> Department of Nuclear Medicine.

<sup>§</sup> Department of Radiology.

<sup>a</sup> Abbreviations: AD, Alzheimer's disease;  $A\beta$ , amyloid  $\beta$ ; BBB, blood–brain barrier; cpm, counts per minute; DMSO, dimethyl sulfoxide; ID, injected dose; ID/g, injected dose per gram tissue; IMPY, 6-iodo-2-(4'-dimethylamino)phenylimidazo[1,2]pyridine; LSO, lutetium oxyorthosilicate; MCI, mild cognitive impairment; Mp, melting point; NFT, neurofibrillary tangle; NMP, *N*-methylpyrrolidone; NMR, nuclear magnetic resonance; *P*, partition coefficient; PBS, phosphate buffered saline; p.i., post injection; PET, positron emission tomography; PPA, polyphosphoric acid; RP-HPLC, reversed phase high performance liquid chromatography;  $t_R$ , retention time; rt, room temperature; SB, stilbene; SD, standard deviation; SEM, standard error of the mean; SUV, standard uptake value; TAC, time–activity curve; THF, tetrahydrofuran; TLC, thin layer chromatography; VOI, volume of interest; DMF, dimethylformide.

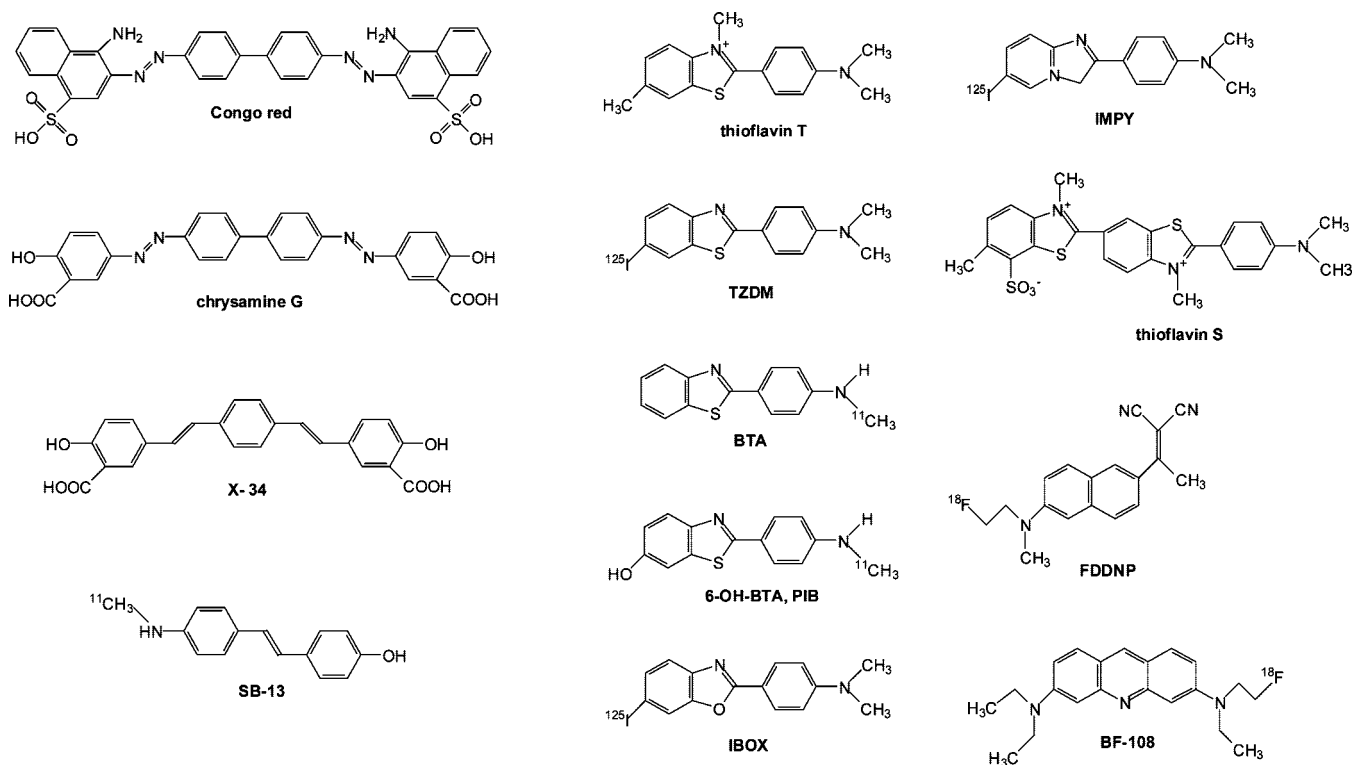
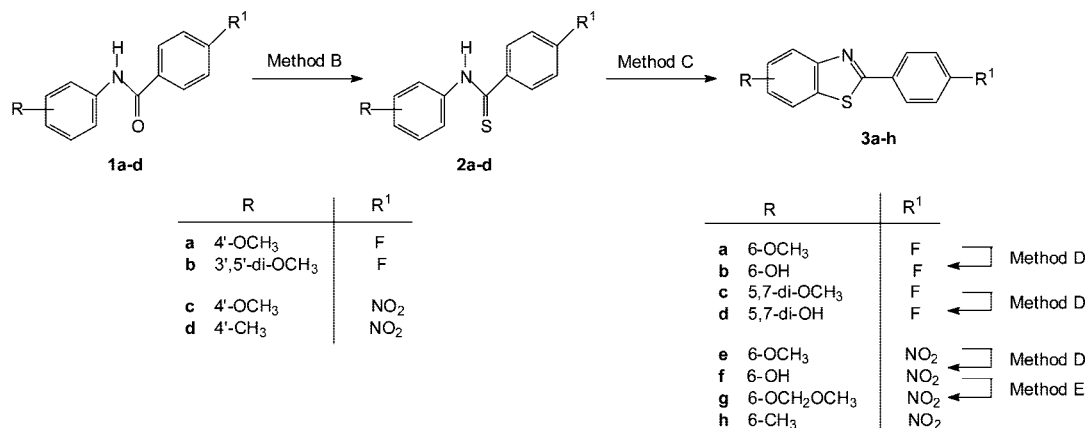


**Figure 1.** Chemical structures of amyloid imaging agents previously reported.

**Scheme 1.** Synthesis of Phenylbenzothiazoles **3a–h**<sup>a</sup>



<sup>a</sup> Method B: Lawesson's reagent, 1,4-dioxane or chlorobenzene, reflux, 3 h. Method C: 10% NaOH, K<sub>3</sub>Fe(CN)<sub>6</sub>, 90 °C, 2 h. Method D: BBr<sub>3</sub>, N<sub>2</sub>, CH<sub>2</sub>Cl<sub>2</sub>, -70 °C, 2 h. Method E: NaH, CH<sub>3</sub>OCH<sub>2</sub>Cl, DMF, rt, 5 h.

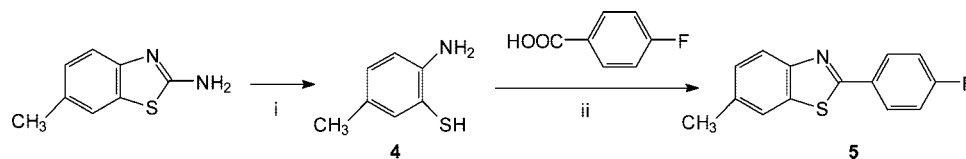
stilbenes,<sup>16</sup> benzothiophenes,<sup>17</sup> biphenyltrienes,<sup>18</sup> styrylbenzenes,<sup>19</sup> styrylpyridines,<sup>20</sup> and curcumin derivatives.<sup>21</sup>

Up to now, by far the most promising and clinically useful results have been obtained with [<sup>11</sup>C]PIB. However, this tracer agent remains suboptimal in view of its labeling with the short-lived carbon-11 (*T*<sub>1/2</sub> = 20.39 min), which limits its availability to centers equipped with a cyclotron. The limitations associated with the short half-life of carbon-11 may be overcome by introducing a fluorine-18 label which has a longer half-life (*T*<sub>1/2</sub> = 109.8 min) and thus may provide a tracer agent that is useful for a widespread clinical application. This paper describes the synthesis, labeling, and biological evaluation of three 2-(4'-[<sup>18</sup>F]fluorophenyl)-1,3-benzothiazoles with the <sup>18</sup>F-label directly attached to the 2-phenyl ring.

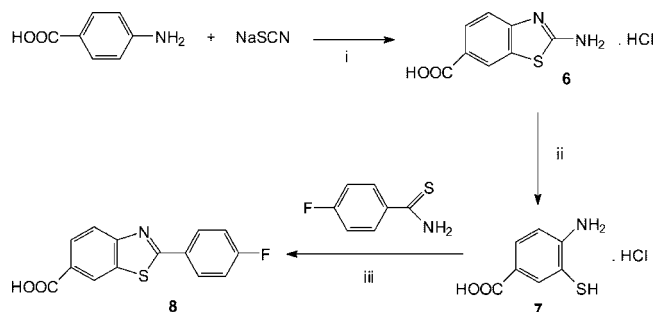
**Results and Discussion**

**Chemistry.** The synthesis of a number of 2-(4'-aminophenyl)-1,3-benzothiazoles has already been described previously.<sup>22–24</sup>

We adapted the described procedures to synthesize the 2-(4'-fluorophenyl)-1,3-benzothiazoles **3a–d** and the nitro precursors **3e–h**. A schematic overview of the synthetic pathways is depicted in Scheme 1. The benzamides **1a–d** were prepared by reaction of the corresponding substituted anilines with 4-fluorobenzoyl chloride or 4-nitrobenzoyl chloride in boiling pyridine (method A). The benzamides were converted to the corresponding thiobenzamides **2a–d** using Lawesson's reagent in 1,4-dioxane (method B). Lawesson's reagent or 2,4-bis(4-methoxyphenyl)-1,3-dithia-2,4-diphosphetane 2,4-disulfide is useful as a thiation reagent to replace the carbonyl oxygen of ketones, amides, and esters with sulfur.<sup>25</sup> For the synthesis of **2b** chlorobenzene was used as solvent, as the conversion in 1,4-dioxane failed. The thiobenzamides were cyclized to their corresponding phenylbenzothiazoles by a Jacobsen synthesis using the oxidizing agent potassium ferricyanide in aqueous sodium hydroxide (method C). Demethylation of the methoxy-

**Scheme 2.** Synthesis of 6-Methyl-2-(4'-fluorophenyl)-1,3-benzothiazole **5**<sup>a</sup>

<sup>a</sup> (i) 50% KOH, reflux, 3 days; (ii) PPA, 220 °C, 4 h.

**Scheme 3.** Synthesis of 6-Carboxy-2-(4'-fluorophenyl)-1,3-benzothiazole **8**<sup>a</sup>

<sup>a</sup> (i) CH<sub>3</sub>OH, Br<sub>2</sub>, -5 °C, 2 h; (ii) KOH, N<sub>2</sub>, reflux, 4 h; (iii) NMP, conc HCl, 100 °C, 8 h.

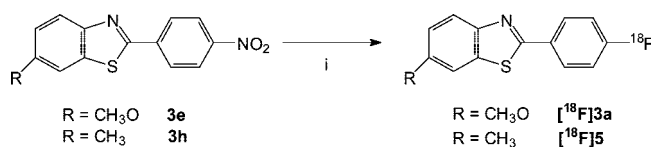
phenylbenzothiazoles **3a**, **3c**, and **3e** was accomplished with excess boron tribromide in dichloromethane at -70 °C to yield the required hydroxylated derivatives **3b**, **3d**, and **3f** (method D).

To protect precursor **3f** with a methoxymethyl protecting group, the compound was first deprotonated using NaH and was then reacted with chloromethyl methyl ether and potassium carbonate at room temperature (rt) (method E, 88% yield).<sup>26</sup> In the absence of sodium hydride only low yields (10%) were obtained even after heating and extended reaction times.

6-Methyl-2-(4'-fluorophenyl)-1,3-benzothiazole (**5**) was synthesized via a direct route<sup>22</sup> by condensation of 2-amino-5-methylthiophenol (**4**), which was synthesized by hydrolytic cleavage of 2-amino-6-methylbenzothiazole with aqueous potassium hydroxide at 100 °C,<sup>27</sup> with commercially available 4-fluorobenzoic acid in polyphosphoric acid (PPA) (Scheme 2). The role of PPA is dual: it serves not only as solvent for the reagents but also as a dehydrating agent, thus shifting the reaction toward the formation of **5**.

6-Carboxy-2-(4'-fluorophenyl)-1,3-benzothiazole (**8**) was synthesized by condensation of 4-amino-3-mercaptobenzoic acid (**7**) with *p*-fluorothiobenzamide in *N*-methylpyrrolidone (NMP) in the presence of 2 equiv of concentrated hydrochloric acid<sup>28</sup> (Scheme 3). 4-Amino-3-mercaptobenzoic acid (**7**) was synthesized following an improved method described by Lang et al.<sup>29</sup> This method does not require stannous chloride to prevent disulfide formation, as the hydrolysis of 2-aminobenzothiazole-6-carboxylic acid (**6**) proceeds in the absence of light and air. **6** was synthesized by adding bromine to a stirred suspension of sodium thiocyanate and 4-aminobenzoic acid.

**Radiochemistry.** To introduce a <sup>18</sup>F-label on the 2-phenyl ring of the phenylbenzothiazoles, an aromatic nucleophilic substitution reaction of the nitro group with [<sup>18</sup>F]fluoride was achieved by heating the solution of the precursor with K[<sup>18</sup>F]F-Kryptofix complex in DMSO at 150 °C for 20 min. Aromatic substitution of a nitro group with fluoride generally requires other electron withdrawing groups on the ortho- or para-position. The presence of an electron withdrawing benzothiazole substituent apparently activates the 4'-nitro group in a sufficient

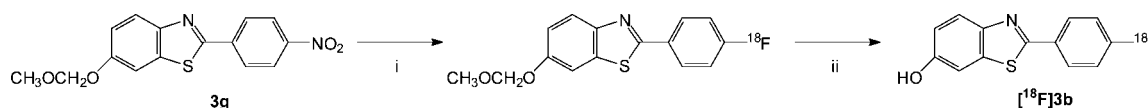
**Scheme 4.** Synthesis of 6-Methoxy-2-(4'-[<sup>18</sup>F]Fluorophenyl)-1,3-benzothiazole [<sup>18</sup>F]**3a** and 6-Methyl-2-(4'-[<sup>18</sup>F]fluorophenyl)-1,3-benzothiazole [<sup>18</sup>F]**5**<sup>a</sup>

<sup>a</sup> (i) <sup>18</sup>F<sup>-</sup>, K<sub>2</sub>CO<sub>3</sub>, Kryptofix, DMSO, 150 °C, 20 min.

way, as relatively high yields of the corresponding [<sup>18</sup>F]fluorophenylbenzothiazoles were obtained (Scheme 4). The labeling of 6-hydroxy-2-(4'-nitrophenyl)-1,3-benzothiazole (**3f**) failed because the alkaline labeling conditions induce a partial negative charge at position 6. As a result, the benzothiazole substituent no longer acts as electron withdrawing substituent but induces a partial negative charge at the N-atom, and therefore, the 4'-nitro group can no longer be substituted by [<sup>18</sup>F]fluoride. To overcome this problem, we introduced a protecting group on the phenol at position 6. The use of an acetate protective group on the phenol was not successful, as labeling of this precursor failed because of instability of the ester in the alkaline labeling conditions. Use of the more stable methoxymethyl protecting group overcame this problem, and labeling of this precursor, 6-methoxymethoxy-2-(4'-nitrophenyl)-1,3-benzothiazole (**3g**), resulted in the corresponding fluorine-18 radiolabeled derivative that was hydrolyzed with a mixture of methanol/concentrated HCl (2:1 v/v) to yield 6-hydroxy-2-(4'-[<sup>18</sup>F]fluorophenyl)-1,3-benzothiazole ([<sup>18</sup>F]**3b**) with a yield of 38% (Scheme 5, Table 1).

Because of the low solubility of the nitro precursors, labeling reactions were performed in dimethyl sulfoxide (DMSO). A rather common challenge for fluorine-18 labeled tracers prepared starting from a nitro precursor is the difficult separation between the nitro precursor and the desired <sup>18</sup>F-labeled compound using high performance liquid chromatography (HPLC). After trying various mobile phase compositions, we found that the use of an XTerra C18 column eluted with an isocratic mixture of 50% 0.05 M NH<sub>4</sub>OAc and 50% ethanol/tetrahydrofuran (THF) (75:25 v/v) allowed an efficient separation for all of the tested compounds. Before purification on preparative HPLC, unreacted [<sup>18</sup>F]F<sup>-</sup> was removed by passing the crude reaction mixture over a Sep-Pak Plus C18 column. The THF present in the HPLC eluent was removed by solid phase extraction using a Sep-Pak Plus C18 cartridge that was first rinsed with water to remove all THF and then eluted with ethanol to provide the pure radiolabeled compound. In a different approach, we synthesized the trimethylammonium precursor of [<sup>18</sup>F]**5** instead of the nitro precursor, but labeling failed because of decomposition of this precursor in the alkaline reaction conditions.

The purified tracer products were analyzed by reversed phase HPLC (RP-HPLC) on an analytical C<sub>18</sub> column employing an isocratic mixture of 50% 0.05 M NH<sub>4</sub>OAc and 50% ethanol/tetrahydrofuran (75:25 v/v) as mobile phase at a flow rate of 1 mL/min. The radiochemical purity was found to be more than

**Scheme 5.** Synthesis of 6-Hydroxy-2-(4'-[<sup>18</sup>F]Fluorophenyl)-1,3-benzothiazole [<sup>18</sup>F]**3b**<sup>a</sup>

<sup>a</sup> (i) <sup>18</sup>F<sup>-</sup>, K<sub>2</sub>CO<sub>3</sub>, Kryptofix, DMSO, 150 °C, 20 min; (ii) CH<sub>3</sub>OH/conc HCl 2:1 v/v, 125 °C, 5 min.

**Table 1.** *K<sub>i</sub>* Values, log *P* Values, and Radiochemical Characteristics of **3a**, **3b**, **3d**, **5**, **8**, and PIB<sup>a</sup>

compd	<i>K<sub>i</sub></i> <sup>b</sup> (nM)	log <i>P</i> <sup>c</sup>	<i>t<sub>R</sub></i> <sup>d</sup> nitro precursor <sup>d</sup> (min)	<i>t<sub>R</sub></i> <sup>d</sup> <sup>18</sup> F product <sup>d</sup> (min)	radiochemical yield <sup>e</sup> (%)
<b>3a</b>	2.2 ± 0.5	2.29 ± 0.24	24	19	24.1 ± 2.3
<b>3b</b>	22.5 ± 4.5	2.73 ± 0.23	24	19	38.0 ± 0.2
<b>3d</b>	776 ± 173	nd	nd	nd	nd
<b>5</b>	5.7 ± 1.8	2.52 ± 0.27	48	41	29.4 ± 3.2
<b>8</b>	>4000	nd	nd	nd	nd
PIB	2.8 ± 0.5	2.48 ± 0.06	nd	nd	nd

<sup>a</sup> nd = not determined. <sup>b</sup> *K<sub>i</sub>* expressed as mean ± SEM (standard error of the mean) in an [<sup>125</sup>I]IMPY competition study (*K<sub>d</sub>* [<sup>125</sup>I]IMPY = 5.3 ± 1.0 nM). <sup>c</sup> log *P* expressed as mean ± SD (standard deviation, *n* = 6). <sup>d</sup> *t<sub>R</sub>* (retention time) determined on HPLC: stationary phase, XTerra Prep RP<sub>18</sub> (10 μm, 10 mm × 250 mm); mobile phase, 0.05 M ammonium acetate and ethanol/THF (75:25) (50:50 v/v); flow rate, 3 mL/min; detection, UV 254 nm. <sup>e</sup> Decay corrected radiochemical yield expressed as mean ± SD (standard deviation, *n* > 3).

95% for each of the compounds. The identity of the tracers was confirmed by co-elution with the authentic nonradioactive compounds after co-injection on the same analytical HPLC system.

**Affinity.** The *in vitro* affinity of the nonradioactive reference compounds for amyloid β fibrils was determined using a [<sup>125</sup>I]IMPY binding competition experiment with human AD brain homogenates. The observed *K<sub>i</sub>* values (Table 1) depend on the nature and position of the substitution groups present on the phenyl ring of the benzothiazole moiety. Compounds **3a**, **3b**, and **5** have a low *K<sub>i</sub>* value and thus show good affinity for Aβ plaques. Substitution of the methoxy group at position 6 in **3a** with a hydroxyl group (**3b**) resulted in a 10-fold lower affinity. Compounds **3d** and **8** only have a low affinity for Aβ plaques. Compounds **3a** and **5** maintained the best affinity values in the nanomolar range of *K<sub>i</sub>* values. Their affinity is comparable with that of <sup>11</sup>C-labeled PIB, which has a *K<sub>i</sub>* value of 2.8 ± 0.5 nM, determined using the same competition assay.

**Partition Coefficient.** As an estimate of the potential of the compounds to cross the BBB by passive diffusion, the lipophilicity of the RP-HPLC purified radiolabeled products was determined by partitioning between 1-octanol and 0.025 M phosphate buffer, pH 7.4 (*n* = 6). The log of the partition coefficient (*P*) values of [<sup>18</sup>F]**3a**, [<sup>18</sup>F]**3b**, and [<sup>18</sup>F]**5** were 2.29 ± 0.24, 2.73 ± 0.23, and 2.52 ± 0.27, respectively (Table 1), and are within the optimal range (log *P* between 1 and 3) for passive diffusion of a compound through the BBB.<sup>30</sup>

**Biodistribution in Normal Mice.** A biodistribution study of [<sup>18</sup>F]**3a**, [<sup>18</sup>F]**3b**, and [<sup>18</sup>F]**5** was performed in normal male NMRI mice at 2 and 60 min post injection (p.i.) to assess the brain pharmacokinetics. Tables 2–4 list the tracer uptake in the most important organs. All compounds showed a relatively high initial brain uptake. The initial uptake in cerebrum of [<sup>18</sup>F]**3a** (5.1 ± 0.4% ID/g) and [<sup>18</sup>F]**5** (5.3 ± 0.7% ID/g) was slightly higher than that of [<sup>18</sup>F]**3b** (4.7 ± 0.5% ID/g). The brain uptake of [<sup>18</sup>F]**5** at 2 min p.i. is significantly higher (*p* < 0.05, two-sided) than that of PIB (Table 5, 3.6 ± 1.4% ID/g). With respect to brain washout (expressed as % ID in cerebrum at 2 min/% ID in cerebrum at 60 min), [<sup>18</sup>F]**5** shows a higher value

**Table 2.** Tissue Distribution of 6-Methoxy-2-(4'-[<sup>18</sup>F]fluorophenyl)-1,3-benzothiazole ([<sup>18</sup>F]**3a**) after iv Injection in Normal Mice at 2 and 60 min p.i. (*n* = 4 at Each Time Point)

organ	% ID ± SD		% ID/g tissue ± SD	
	2 min p.i.	60 min p.i.	2 min p.i.	60 min p.i.
urine	0.2 ± 0.2	16.9 ± 8.6		
kidneys	8.6 ± 0.8	9.4 ± 6.5	13.9 ± 0.9	14.2 ± 9.6
liver	19.9 ± 2.4	13.6 ± 3.6	9.9 ± 1.1	6.7 ± 2.2
spleen + pancreas	1.3 ± 0.2	0.2 ± 0.0	4.1 ± 0.3	0.4 ± 0.1
lungs	2.3 ± 0.2	0.6 ± 0.3	9.9 ± 1.2	2.1 ± 0.8
heart	0.8 ± 0.2	0.1 ± 0.0	3.9 ± 1.4	0.6 ± 0.2
intestines	8.4 ± 0.6	34.3 ± 6.1		
stomach	1.1 ± 0.3	1.2 ± 0.8		
cerebrum	1.57 ± 0.18	0.13 ± 0.04	5.10 ± 0.40	0.43 ± 0.12
cerebellum	0.56 ± 0.11	0.07 ± 0.04	5.12 ± 0.51	0.68 ± 0.29
blood	4.9 ± 1.8	4.4 ± 1.8	2.0 ± 0.8	1.7 ± 0.6

**Table 3.** Tissue Distribution of 6-Hydroxy-2-(4'-[<sup>18</sup>F]fluorophenyl)-1,3-benzothiazole ([<sup>18</sup>F]**3b**) after iv Injection in Normal Mice at 2 and 60 min p.i. (*n* = 3 at Each Time Point)

organ	% ID ± SD		% ID/g tissue ± SD	
	2 min p.i.	60 min p.i.	2 min p.i.	60 min p.i.
urine	0.1 ± 0.1	11.3 ± 2.4		
kidneys	7.0 ± 1.0	5.9 ± 0.6	12.6 ± 1.4	11.8 ± 2.6
liver	28.1 ± 1.6	24.6 ± 9.3	13.3 ± 0.7	11.9 ± 4.5
spleen + pancreas	1.2 ± 0.1	0.5 ± 0.3	4.0 ± 0.1	1.8 ± 0.7
lungs	7.6 ± 2.1	1.5 ± 0.4	28.1 ± 3.6	5.5 ± 2.0
heart	0.9 ± 0.2	0.1 ± 0.0	5.8 ± 1.1	1.3 ± 1.4
intestines	7.1 ± 0.7	36.7 ± 10.6		
stomach	1.1 ± 0.2	0.5 ± 0.1		
cerebrum	1.35 ± 0.25	0.16 ± 0.10	4.70 ± 0.48	0.57 ± 0.36
cerebellum	0.55 ± 0.07	0.08 ± 0.07	5.13 ± 0.54	0.76 ± 0.49
blood	10.0 ± 3.7	3.3 ± 2.8	4.0 ± 1.6	1.3 ± 1.1

**Table 4.** Tissue Distribution of 6-Methyl-2-(4'-[<sup>18</sup>F]fluorophenyl)-1,3-benzothiazole ([<sup>18</sup>F]**5**) after iv Injection in Normal Mice at 2 and 60 min p.i. (*n* = 6 at Each Time Point)

organ	% ID ± SD		% ID/g tissue ± SD	
	2 min p.i.	60 min p.i.	2 min p.i.	60 min p.i.
urine	0.2 ± 0.1	3.3 ± 1.8		
kidneys	5.8 ± 1.4	2.3 ± 0.2	9.3 ± 2.0	3.6 ± 0.4
liver	24.8 ± 3.3	51.8 ± 1.8	12.0 ± 0.7	24.6 ± 2.1
spleen + pancreas	1.3 ± 0.2	0.1 ± 0.0	4.0 ± 0.7	0.4 ± 0.1
lungs	3.6 ± 1.0	0.3 ± 0.1	14.4 ± 2.0	1.3 ± 0.2
heart	0.9 ± 0.1	0.1 ± 0.0	5.4 ± 0.5	0.5 ± 0.1
intestines	8.9 ± 1.0	19.3 ± 1.3		
stomach	1.3 ± 0.2	1.1 ± 0.6		
cerebrum	1.62 ± 0.29	0.07 ± 0.02	5.33 ± 0.74	0.27 ± 0.06
cerebellum	0.42 ± 0.16	0.04 ± 0.02	5.99 ± 0.70	0.39 ± 0.06
blood	5.7 ± 2.4	2.8 ± 2.2	2.2 ± 0.9	1.1 ± 0.9

(23.1) than [<sup>18</sup>F]**3a** (12.1) and [<sup>18</sup>F]**3b** (8.4). In healthy mice, a compound with favorable characteristics for plaque imaging should not only have a high affinity for amyloid but also show a high initial brain uptake followed by a rapid washout, indicating absence of nonspecific binding to any brain structure devoid of amyloid plaques. Compound [<sup>18</sup>F]**5** with the highest initial brain uptake and the fastest brain washout value, which is almost 4 times higher than that of [<sup>11</sup>C]PIB, seems to be the

**Table 5.** Tissue Distribution of 6-Hydroxy-2-(4'-N-[<sup>11</sup>C]methyl-aminophenyl)-1,3-benzothiazole ([<sup>11</sup>C]PIB) after iv Injection in Normal Mice at 2 and 60 min p.i. (*n* = 6 at Each Time Point)

organ	% ID ± SD		% ID/g tissue ± SD	
	2 min p.i.	60 min p.i.	2 min p.i.	60 min p.i.
urine	0.2 ± 0.1	24.4 ± 10.1		
kidneys	10.3 ± 3.8	4.8 ± 3.9	19.9 ± 9.1	9.1 ± 7.1
liver	15.6 ± 4.5	9.8 ± 2.6	7.9 ± 2.6	5.0 ± 1.7
spleen + pancreas	0.6 ± 0.1	0.1 ± 0.1	4.7 ± 2.4	0.7 ± 0.4
lungs	0.9 ± 0.2	0.3 ± 0.2	3.6 ± 0.6	1.3 ± 0.7
heart	0.6 ± 0.1	0.3 ± 0.2	4.2 ± 0.3	2.1 ± 2.1
intestines	12.0 ± 2.4	42.5 ± 7.5		
stomach	1.1 ± 0.2	0.3 ± 0.2		
cerebrum	1.08 ± 0.44	0.18 ± 0.06	3.60 ± 1.40	0.60 ± 0.21
cerebellum	0.17 ± 0.02	0.03 ± 0.02	1.60 ± 0.09	0.31 ± 0.13
blood	7.9 ± 0.5	2.7 ± 0.8	3.1 ± 0.2	1.1 ± 0.3

compound with the most promising characteristics to image AD in vivo. The new <sup>18</sup>F-labeled 2-phenylbenzothiazoles do not show a significant difference between the uptake in the cerebrum and cerebellum, whereas [<sup>11</sup>C]PIB does. As the cerebellum contains more white matter, it is possible that the <sup>18</sup>F-labeled 2-phenylbenzothiazoles bind more to the white matter of the brain. The consequence of this with respect to imaging may be a lower signal/noise ratio because there may be more white matter retention. Blood levels of the three compounds were relatively low at all time points measured. Clearance of [<sup>18</sup>F]**5** from the blood (expressed as % ID in blood at 2 min/% ID in blood at 60 min, 2.0) was between the clearance values of [<sup>18</sup>F]**3a** (1.1) and [<sup>18</sup>F]**3b** (3.0) and in the same range as that of PIB (2.9). The distribution of these tracer agents in other organs is of a lesser concern. As could be expected from the relatively high log *P* value, the compounds were cleared mainly by the hepatobiliary system (ranging from 48% ID for the methoxy derivative to 71% ID for the methyl derivative at 60 min p.i.) and to a lesser extent to the urine (ranging from 5.6% ID for the methyl derivative to 26% ID for the methoxy derivative at 60 min p.i.). Except for the liver, intestines, and kidneys, the amount of radioactivity in other major organs was negligible 60 min after injection of the tracers. This indicates a good clearance of the tracer agents from the major organs.

**μPET Study in a Normal Rat.** To compare the brain pharmacokinetics of [<sup>18</sup>F]**3a**, [<sup>18</sup>F]**3b**, and [<sup>18</sup>F]**5** with those of [<sup>11</sup>C]PIB, the compounds were also injected in a normal rat and μPET images were acquired for 120 min. Figure 2 shows the time–activity curves (TACs) for [<sup>18</sup>F]**3a**, [<sup>18</sup>F]**3b**, and [<sup>18</sup>F]**5** and [<sup>11</sup>C]PIB in the frontotemporal cortex of a normal rat. Values are expressed as standard uptake values (SUVs).

The tested fluorine-18 labeled PIB derivatives all showed a similar initial brain uptake followed by a relatively rapid washout comparable with that of [<sup>11</sup>C]PIB. The lower variability of the brain pharmacokinetics of the tested compounds observed in rats compared to the values observed in mice may be explained by interspecies differences. As no tracer uptake was observed in the skull, we can conclude that the new <sup>18</sup>F-labeled 2-phenylbenzothiazoles do not show substantial defluorination in vivo.

**Biostability of [<sup>18</sup>F]**5** in Normal Mice.** Because [<sup>18</sup>F]**5** showed the most promising results (highest brain uptake and fastest washout in normal mice), the in vivo metabolic stability of [<sup>18</sup>F]**5** was studied by analyzing plasma and brain of normal mice after injection of [<sup>18</sup>F]**5** using RP-HPLC analysis. The nonradioactive reference compound **5** was co-injected on HPLC to assess the retention time of intact parent tracer.

For the analysis, online solid phase extraction using an Oasis HLB column was employed. After injection of the samples on

the Oasis column, the proteins and other hydrophilic matrix components were washed from the column using water. The analytes were then eluted from the Oasis column and led over a reversed phase analytical column, the eluate of which was collected in 1.5 mL fractions followed by counting of all fractions for radioactivity.<sup>31</sup> The recoveries of HPLC/Oasis column injected radioactivity during these analyses were found to be high with mean recovery of 82.0 ± 4.1% (*n* = 6). An example of plasma analysis is shown in Figure 3. Table 6 shows the percentage of intact [<sup>18</sup>F]**5** in plasma of normal mice as a function of time. At 2 min p.i., already 40% of the tracer agent was converted into at least three unidentified radiolabeled polar metabolites. At 60 min p.i., only 1.6% of the intact compound was found. This was not the case with [<sup>11</sup>C]PIB, which is much more stable, with more than 80% intact tracer in plasma at 60 min p.i. (data not shown). Only relatively low amounts (<15%) of radiometabolites were found in the brain at 2 or 60 min p.i. (% intact tracer at 2 min p.i., 89.2 ± 0.4; % intact tracer at 60 min p.i., 86.2 ± 2.5; *n* = 2), indicating that no substantial metabolism of [<sup>18</sup>F]**5** occurs in brain and that its radiometabolites do not cross the BBB to a high extent in mice.

**Biostability in Brain of a Normal Rat.** After intravenous injection of [<sup>18</sup>F]**5** in a normal rat, a polar radiolabeled metabolite that reached 22% of the total radioactivity was observed in brain at 2 min p.i. (78.4% intact tracer, *n* = 1). These findings are in agreement with the reported formation of a radiolabeled metabolite of [<sup>11</sup>C]PIB, namely, 6-sulfato-PIB, in rat brain, but also for this compound no radiometabolites were formed in mouse or human brain homogenates.<sup>32</sup> This similar biological behavior of [<sup>11</sup>C]PIB and [<sup>18</sup>F]**5** suggests that replacement of the *N*-methyl substituent on the 2-phenyl ring of PIB by a fluorine atom does not affect significantly the pharmacokinetics. The only difference is the slightly higher relative uptake in the cerebellum.

## Conclusion

To allow noninvasive in vivo imaging of amyloid plaques for early stage diagnosis of Alzheimer's disease and monitoring of the disease progression and treatment efficacy with PET, the search for a clinically useful radiolabeled derivative of thioflavin-T has become a subject of worldwide research. Up to now, by far the most promising and clinically useful results have been obtained with [<sup>11</sup>C]PIB. The limitations associated with the short half-life of carbon-11 may be overcome by introducing a fluorine-18 label and thus may provide a tracer agent that is useful for a widespread clinical application.

We synthesized five 2-(4'-fluorophenyl)-1,3-benzothiazoles of which three show high in vitro affinity for amyloid plaques present in human AD post mortem brain homogenates. The corresponding nitro precursors were synthesized, and successful <sup>18</sup>F-labeling was performed by heating for 20 min at 150 °C in DMSO. The studied <sup>18</sup>F-labeled phenylbenzothiazoles show a log *P* value between 2.2 and 2.8. Their ability to pass the blood–brain barrier was confirmed by a biodistribution study in normal mice. All compounds show a high initial uptake in cerebrum of normal mice. Compound [<sup>18</sup>F]**5** has the highest brain uptake, significantly higher than that of the <sup>11</sup>C-labeled PIB. The compound also showed a faster brain washout than [<sup>11</sup>C]PIB. In vivo biostability of [<sup>18</sup>F]**5** was studied in plasma and brain of normal mice. The compound was extensively metabolized, as large amounts of three unidentified radiolabeled polar metabolites were found in plasma but not in brain. These preliminary results strongly suggest that this new fluorinated

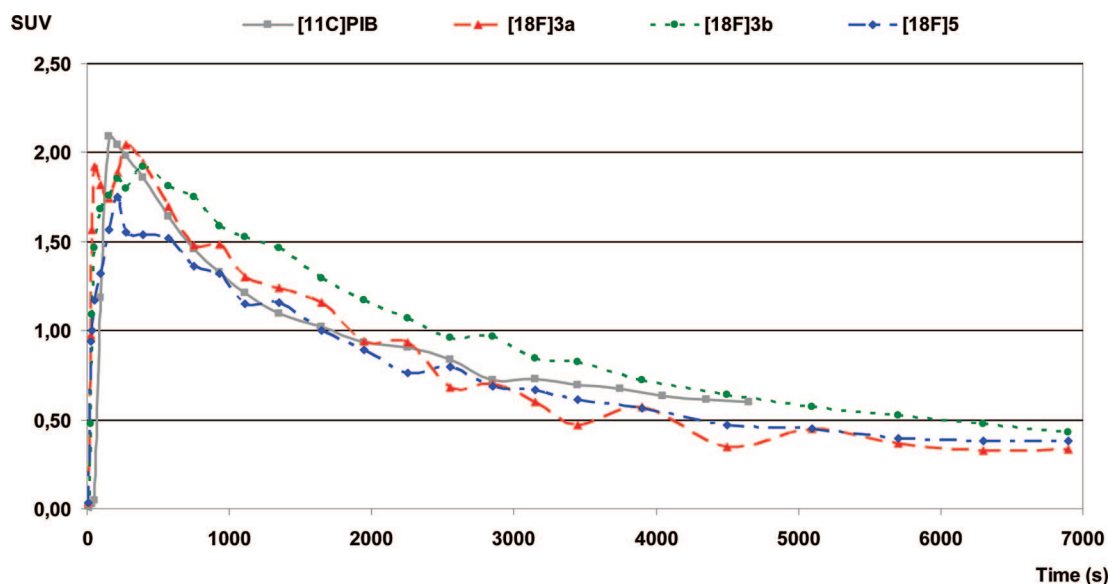


**Figure 2.** Standard uptake values (SUVs) of [<sup>18</sup>F]3a, [<sup>18</sup>F]3b, and [<sup>18</sup>F]5 and [<sup>11</sup>C]PIB in the frontotemporal cortex of a normal rat.

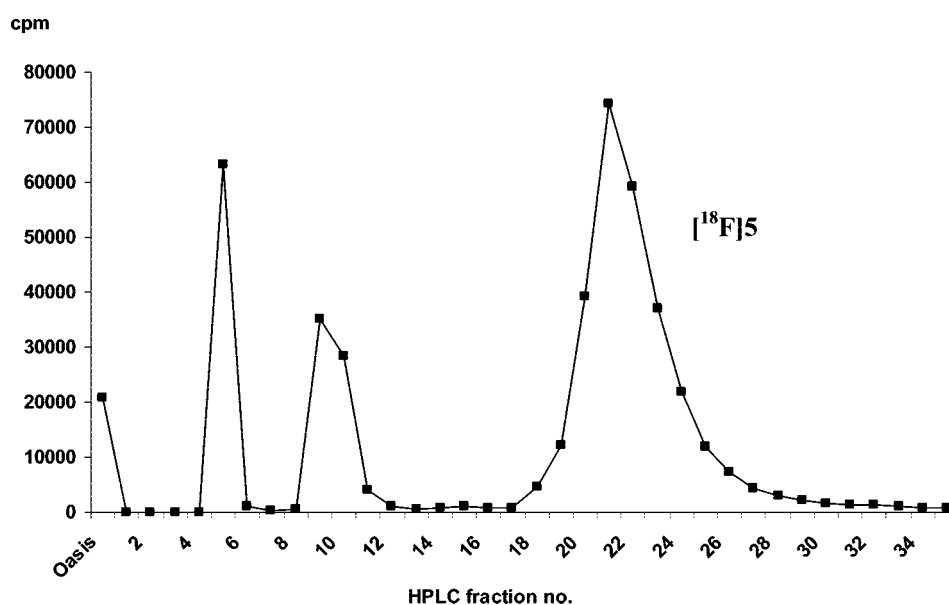


**Figure 3.** Plasma radiometabolite analysis of [<sup>18</sup>F]5: RP-HPLC radiochromatogram of a plasma sample from a normal mouse collected 2 min p.i. The 1 min fractions were collected and counted.

**Table 6.** Percentage of Intact [<sup>18</sup>F]5 in Plasma of Normal Mice at 2, 10, 30, and 60 min p.i. (*n* = 3 at Each Time Point)

time (min)	% intact	SD
2	52.15	13.15
10	13.95	6.23
30	7.88	2.80
60	3.19	1.66

compound is a promising candidate as a A $\beta$  plaque imaging agent for studying patients with AD.

## Experimental Section

**Chemicals and Reagents.** *p*-Anisidine, 4-fluorobenzoyl chloride, 4-nitrobenzoyl chloride, and *p*-toluidine were obtained from Acros Organics (Geel, Belgium). 2-Amino-6-methylbenzothiazole and ethyl 4-aminobenzoate were obtained from Aldrich (Sigma-Aldrich, Bornem, Belgium). 4-Fluorobenzoic acid was purchased from Avocado (Karlsruhe, Germany). 3,5-Dimethoxyaniline was obtained from Fluka (Bornem, Belgium). All other reagents and solvents

were obtained commercially from Acros Organics, Fischer Bioblock Scientific (Tournai, Belgium), Fluka, Merck (Darmstadt, Germany), or Riedel-de Haën (Seelze, Germany). They were all used without further purification.

**Apparatus, Instruments, and General Conditions.** MgSO<sub>4</sub> was used as drying agent. pH values of nonradioactive solutions were measured with a P600 pH meter (Consort, Turnhout, Belgium) provided with a glass electrode. pH determination of radioactive solutions was done with pH strips (pH strips 0–14, Merck, Darmstadt, Germany). Evaporation of organic solvents under reduced pressure was done with a Büchi rotovapor (Büchi, Flawil, Switzerland). Purification of reaction mixtures was done by column chromatography using silica gel with a particle size varying between 0.04 and 0.063 mm (230–400 mesh, MN Kieselgel 60M, Macherey-Nagel, Düren, Germany) as the stationary phase. Thin layer chromatography (TLC) was done on precoated silica TLC plates (DC-Alufohlen-Kieselgel, Fluka, Buchs, Switzerland). The structures of the synthesized products were confirmed with <sup>1</sup>H nuclear magnetic resonance (NMR) spectroscopy on a Gemini 200 MHz spectrometer (Varian, Palo Alto, CA) or a Bruker AVANCE 300

MHz spectrometer (Bruker AG, Faellanden, Switzerland). Chemical shifts are reported as  $\delta$ -values (parts per million) relative to tetramethylsilane ( $\delta = 0$ ). Coupling constants are reported in hertz. Splitting patterns are defined by s (singlet), d (doublet), dd (double doublet), t (triplet), and m (multiplet). Melting points (Mp's) were determined with an IA9100 digital melting point apparatus (Electrothermal, Essex, U.K.) in open capillaries and are reported uncorrected. Exact mass measurement was performed on a time-of-flight mass spectrometer (LCT, Micromass, Manchester, U.K.) equipped with an orthogonal electrospray ionization interface and operating in positive mode ( $ES^+$ ). Accurate mass determination was done by co-injection with a compound with known mass as an internal calibration standard (lock mass). Acquisition and processing of data were done using Masslynx software (version 3.5, Waters).

Reversed phase high performance liquid chromatography (RP-HPLC) purification and analysis were performed either on a Merck Hitachi L6200 pump (Hitachi, Tokyo, Japan) or on a Waters 600 pump (Waters, Milford) connected to a UV spectrometer (Waters 2487 dual  $\lambda$  absorbance detector). The output signal was recorded and analyzed using a RaChel data acquisition system (Lablogic, Sheffield, U.K.). For analysis of radiolabeled compounds, the HPLC eluate was led over a 3 in. NaI(Tl) scintillation detector connected to a single channel analyzer (Medi-Laboratory Select, Mechelen, Belgium) after passing through an UV detector.

Gas chromatography was performed on a DI 200 gas chromatograph (Delsi Instruments, Suresnes, France) with a Porapak QS 80/100 column (Alltech, Deerfield, IL) of 180 cm  $\times$  0.25 in.

Animal studies were performed according to the Belgian code of practice for the care and use of animals, after approval from the university ethics committee for animals.

[ $^{11}C$ ]PIB was synthesized using [ $^{11}C$ ]methyl triflate following a described procedure.<sup>33</sup>

Quantitative determination of radioactivity in samples was done using an automatic  $\gamma$ -counter coupled to a multichannel analyzer (Wallac 1480 Wizard 3", Wallac, Turku, Finland). The results were corrected for background radiation and physical decay during counting.

Dynamic  $\mu$ PET imaging was performed using a lutetium oxyorthosilicate (LSO) detector-based tomograph (microPET Focus 220; Siemens Medical Solutions, Knoxville, TN), which has a transaxial resolution of 1.35 mm in full width at half-maximum. Data were acquired in a 128  $\times$  128  $\times$  95 matrix with a pixel width of 0.475 mm and a slice thickness of 0.796 mm. The coincidence window width was set at 6 ns.

#### Synthesis. *N*-4'-Methoxyphenyl-4-fluorobenzamide (**1a**).

**Method A.** A solution of *p*-anisidine (16.50 g, 0.134 mol) and 4-fluorobenzoyl chloride (21.25 g, 0.134 mol) in 70 mL of pyridine was refluxed for 1 h. After cooling to room temperature (rt), the mixture was poured into water and the precipitate was filtered off, washed with water, and dried in a vacuum oven. Crystallization from methanol yielded 26.73 g of **1a** as white crystals (0.109 mol, 81%).  $^1H$  NMR (DMSO- $d_6$ , 200 MHz):  $\delta$  3.73 (s, 3H,  $CH_3O$ ),  $\delta$  6.92 (dd, 2H,  $^3J = 7.0$  Hz,  $^4J = 2.2$  Hz, 3'-H 5'-H),  $\delta$  7.33 (t, 2H,  $^3J = 9.0$  Hz, 3-H 5-H),  $\delta$  7.64 (dd, 2H,  $^3J = 9.2$  Hz,  $^4J = 2.2$  Hz, 2'-H 6'-H),  $\delta$  8.01 (dd, 2H,  $^3J = 8.8$  Hz,  $^4J = 3.2$  Hz, 2-H 6-H),  $\delta$  10.16 (s, 1H, NH-CO). Accurate MS  $ES^+ m/z$  [M + H] $^+$  246.0912 (calculated for  $C_{14}H_{12}NO_2F$  246.0925). Mp: 185.6–186.2  $^{\circ}C$ .

#### *N*-4'-Methoxyphenyl-4-fluorothiobenzamide (**2a**). Method

**B.** A solution of **1a** (21.83 g, 0.089 mol) and Lawesson's reagent (16.18 g, 0.040 mol) in 1,4-dioxane (130 mL) was heated under reflux for 3 h, after which it was cooled to room temperature and poured into water. The precipitate was filtered off, washed with water, and dried in a vacuum oven. Crystallization from methanol yielded 17.84 g of **2a** as yellow needles (0.068 mol, 76%).  $^1H$  NMR (DMSO- $d_6$ , 200 MHz):  $\delta$  3.77 (s, 3H,  $CH_3O$ ),  $\delta$  6.97 (dd, 2H,  $^3J = 7.0$  Hz,  $^4J = 2.2$  Hz, 3'-H 5'-H),  $\delta$  7.28 (t, 2H,  $^3J = 8.3$  Hz, 3-H 5-H),  $\delta$  7.67 (dd, 2H,  $^3J = 6.8$  Hz,  $^4J = 2.4$  Hz, 2'-H 6'-H),  $\delta$  7.90 (dd, 2H,  $^3J = 7.7$  Hz,  $^4J = 3.2$  Hz, 2-H 6-H),  $\delta$  10.16 (s, 1H, NH-CS). Accurate MS  $ES^+ m/z$  [M + H] $^+$  262.0681 (calculated for  $C_{14}H_{12}NOFS$  262.0696). Mp: 159.2–159.6  $^{\circ}C$ .

**6-Methoxy-2-(4'-fluorophenyl)-1,3-benzothiazole (3a). Method C.** A solution of **2a** (13.06 g, 0.050 mol) in a mixture of ethanol (20 mL) and 10% (mol/v) sodium hydroxide (100 mL) was slowly added over a period of 2 h to a solution of potassium ferricyanide (65.85 g, 0.200 mol) in water (125 mL) at 90  $^{\circ}C$ . The obtained suspension was stirred for 2 h at 90  $^{\circ}C$  and then cooled to 4  $^{\circ}C$ . The precipitate was filtered off, washed with water, and dried in a vacuum oven. The dry residue was dispersed in a mixture of dichloromethane/ethanol (75:25 v/v, 1 L). The dispersion was filtered off, and the filtrate was concentrated by vacuum evaporation. The residue was purified with silica column chromatography using gradient mixtures of hexane and ethyl acetate (up to 50%) as eluent to yield 1.29 g of **3a** as a yellow solid (0.005 mol, 10%).  $^1H$  NMR ( $CDCl_3$ , 200 MHz):  $\delta$  3.89 (s, 3H,  $CH_3O$ ),  $\delta$  7.09 (dd, 1H,  $^3J = 8.7$  Hz,  $^4J = 2.4$  Hz, 5-H),  $\delta$  7.16 (t, 2H,  $^3J = 8.8$  Hz, 3'-H 5'-H),  $\delta$  7.34 (d, 1H,  $^4J = 2.6$  Hz, 7-H),  $\delta$  7.93 (d, 1H,  $^3J = 8.8$  Hz, 4-H),  $\delta$  8.02 (dd, 2H,  $^3J = 7.8$  Hz,  $^4J = 3.6$  Hz, 2'-H 6'-H). Accurate MS  $ES^+ m/z$  [M + H] $^+$  260.0536 (calculated for  $C_{14}H_{10}NOFS$  260.0540). Mp: 180.5–181.2  $^{\circ}C$ .

**6-Hydroxy-2-(4'-fluorophenyl)-1,3-benzothiazole (3b). Method D.** A dispersion of **3a** (1.56 g, 0.0060 mol) in dichloromethane (60 mL) was cooled to  $-70$   $^{\circ}C$  under nitrogen. Over a period of 1 h, 0.027 mol of  $BBr_3$  (27 mL of a 1 M solution in dichloromethane) was added slowly, after which the mixture was stirred for another hour at  $-70$   $^{\circ}C$ . The suspension was allowed to warm to room temperature and was stirred for 45 h. The suspension was cooled to  $-70$   $^{\circ}C$ , and methanol (60 mL) was added slowly until no more gas evolved. After warming to room temperature, the suspension was extracted three times with 2 M sodium hydroxide (100 mL). The aqueous layer was separated and neutralized with 6 M hydrochloric acid and again extracted three times with a mixture of dichloromethane/methanol (4:1 v/v, 200 mL). The combined organic layers were dried over  $MgSO_4$ , filtered, and evaporated to dryness. Crystallization from methanol yielded 1.22 g of **3b** (0.0050 mol, 83%) as white crystals.  $^1H$  NMR (DMSO- $d_6$ , 200 MHz):  $\delta$  7.00 (dd, 1H,  $^3J = 8.8$  Hz,  $^4J = 2.2$  Hz, 5-H),  $\delta$  7.37 (t, 2H,  $^3J = 8.8$  Hz, 3'-H 5'-H),  $\delta$  7.41 (d, 1H,  $^4J = 2.2$  Hz, 7-H),  $\delta$  7.85 (d, 1H,  $^3J = 8.8$  Hz, 4-H),  $\delta$  8.05 (dd, 2H,  $^3J = 7.7$  Hz,  $^4J = 3.2$  Hz, 2'-H 6'-H),  $\delta$  9.91 (s, 1H, OH). Accurate MS  $ES^+ m/z$  [M + H] $^+$  246.0361 (calculated for  $C_{13}H_8NOFS$  246.0383). Mp: 224.0–224.8  $^{\circ}C$ .

#### 6-Methoxymethoxy-2-(4'-nitrophenyl)-1,3-benzothiazole (3g).

**Method E.** To a solution of **3f** (0.44 g, 0.0016 mol) in dry dimethylformide (DMF) (15 mL) was added slowly NaH (0.043 g, 0.0018 mol), and the resulting mixture was stirred at room temperature for 30 min. After cooling the reaction mixture to 0  $^{\circ}C$ , chloromethyl methyl ether (0.5 mL, 0.0066 mol) was added and the pH of the reaction mixture was adjusted to 9 using potassium carbonate (2 g, 0.014 mol). After being stirred at room temperature for 5 h, the reaction mixture was poured into water and extracted with ethyl acetate. The organic layer was dried over  $MgSO_4$ , filtered, and evaporated to dryness. The residue was purified with silica column chromatography using a mixture of ethyl acetate and hexane (1:3 v/v) as eluent to yield 0.46 g of **3g** as a yellow solid (0.0014 mol, 88%).  $^1H$  NMR ( $CDCl_3$ , 200 MHz):  $\delta$  3.46 (s, 3H,  $CH_3O$ ),  $\delta$  5.19 (s, 2H,  $CH_2O$ ),  $\delta$  7.16 (dd, 1H,  $^3J = 8.8$  Hz,  $^4J = 2.2$  Hz, 5-H),  $\delta$  7.53 (d, 1H,  $^4J = 2.2$  Hz, 7-H),  $\delta$  7.93 (d, 1H,  $^3J = 8.8$  Hz, 4-H),  $\delta$  8.12 (dd, 2H,  $^3J = 6.8$  Hz,  $^4J = 2.0$  Hz, 2'-H 6'-H),  $\delta$  8.25 (d, 2H,  $^3J = 6.8$  Hz,  $^4J = 2.4$  Hz, 3'-H 5'-H). Accurate MS  $ES^+ m/z$  [M + H] $^+$  317.0576 (calculated for  $C_{15}H_{12}N_2O_4S$  317.0591). Mp: 133.3–133.5  $^{\circ}C$ .

**2-Amino-5-methylthiophenol (4).** A mixture of 2-amino-6-methylbenzothiazole (13.14 g, 0.080 mol) and 50% (mol/v) KOH (800 mL) was refluxed during 3 days. The reaction mixture was poured into water, and acetic acid was added to attain pH 6.5. The yellow precipitate was extracted with ethyl acetate, dried over  $MgSO_4$ , filtered, and evaporated to dryness. The resulting residue was purified with silica column chromatography using dichloromethane as eluent to yield 5.98 g of **4** as a yellow solid (0.043 mol, 54%).  $^1H$  NMR ( $CDCl_3$ , 200 MHz):  $\delta$  2.13 (s, 3H,  $CH_3$ ),  $\delta$  4.17 (s, 2H,  $NH_2$ ),  $\delta$  6.63 (d, 1H,  $^3J = 8.0$  Hz, 3-H),  $\delta$  6.95 (s, 1H,

4-H),  $\delta$  6.99 (d, 1H,  $^4J = 2.2$  Hz, 6-H). Accurate MS ES<sup>+</sup>  $m/z$  [M + H]<sup>+</sup> 140.0528 (calculated for C<sub>7</sub>H<sub>9</sub>NS 140.0522). Mp: 85.8–87.3 °C.

**6-Methyl-2-(4'-fluorophenyl)-1,3-benzothiazole (5).** A mixture of **4** (2.78 g, 0.02 mol) and 4-fluorobenzoic acid (2.80 g, 0.02 mol) in polyphosphoric acid (PPA, 75 g) was stirred at 220 °C for 4 h. After cooling to room temperature, the reaction mixture was poured into a 10% (mol/v) Na<sub>2</sub>CO<sub>3</sub> solution. The precipitate was filtered off, washed with water, and dried in a vacuum oven. The residue was purified with silica column chromatography using gradient mixtures of hexane and ethyl acetate (up to 10%) as eluent to yield 0.64 g of **5** as a yellow solid (0.0026 mol, 13%). <sup>1</sup>H NMR (CDCl<sub>3</sub>, 300 MHz):  $\delta$  2.47 (s, 3H, CH<sub>3</sub>),  $\delta$  7.14 (t, 2H,  $^3J = 8.6$  Hz, 3'-H 5'-H),  $\delta$  7.28 (dd, 1H,  $^3J = 8.4$  Hz,  $^4J = 1.4$  Hz, 5-H),  $\delta$  7.65 (s, 1H, 7-H),  $\delta$  7.91 (d, 1H,  $^3J = 8.6$  Hz, 4-H),  $\delta$  8.03 (dd, 2H,  $^3J = 7.8$  Hz,  $^4J = 3.6$  Hz, 2'-H 6'-H). Accurate MS ES<sup>+</sup>  $m/z$  [M + H]<sup>+</sup> 244.0498 (calculated for C<sub>14</sub>H<sub>10</sub>FNS 244.0591). Mp: 150.0–150.9 °C.

**2-Aminobenzothiazole-6-carboxylic Acid Hydrochloride (6).** To a stirred suspension of sodium thiocyanate (13.00 g, 0.160 mol) and 4-aminobenzoic acid (20.00 g, 0.146 mol) in methanol (75 mL) was slowly added bromine (7.5 mL, 0.146 mol) while the temperature was maintained below –5 °C. After addition, the mixture was stirred for 2 h at the same temperature. The precipitated solid was collected and washed with water. The isolated solid was suspended in hydrochloric acid (1 M, 70 mL), and the suspension was refluxed for 30 min and then filtered while hot. Concentrated hydrochloric acid (30 mL) was added to the filtrate, producing a white solid after cooling in a refrigerator. The white solid was collected and dried under vacuum to yield 21.59 g of **6** (0.094 mol, 64%). The crude product was used without further purification. <sup>1</sup>H NMR (DMSO-*d*<sub>6</sub>, 200 MHz):  $\delta$  7.60 (d, 1H,  $^3J = 8.8$  Hz, 4-H),  $\delta$  7.80 (dd, 1H,  $^3J = 8.5$  Hz,  $^4J = 1.9$  Hz, 5-H),  $\delta$  8.51 (d, 1H,  $^4J = 1.6$  Hz, 7-H). Accurate MS ES<sup>+</sup>  $m/z$  [M + H]<sup>+</sup> 195.0217 (calculated for C<sub>8</sub>H<sub>6</sub>N<sub>2</sub>O<sub>2</sub>S 195.0223). Mp: 294.2–295.7 °C.

**4-Amino-3-mercaptopbenzoic Acid Hydrochloride (7).** A suspension of **6** (6.00 g, 0.026 mol) and potassium hydroxide (26.32 g, 0.496 mol) in degassed demineralized water (50 mL) was shielded from light (aluminum foil) and then refluxed under nitrogen for 4 h. After the mixture was cooled to room temperature, concentrated hydrochloric acid (45 mL) was added dropwise under nitrogen. The resulting mixture was cooled to 5 °C and stirred for 30 min. The precipitate was collected under a nitrogen blanket and dried under vacuum to give 4.14 g of the desired product **7** as a white solid (0.024 mol, 92%). The product was stored under light- and oxygen-free conditions (–5 °C). <sup>1</sup>H NMR (DMSO-*d*<sub>6</sub>, 200 MHz):  $\delta$  6.76 (d, 1H,  $^3J = 8.4$  Hz, 5-H),  $\delta$  7.46 (d, 1H,  $^4J = 2.2$  Hz, 2-H),  $\delta$  7.62 (dd, 1H,  $^3J = 8.6$  Hz,  $^4J = 2.0$  Hz, 6-H). Accurate MS ES<sup>+</sup>  $m/z$  [M + H]<sup>+</sup> 170.0284 (calculated for C<sub>7</sub>H<sub>7</sub>NO<sub>2</sub>S 170.0270). Mp: 288.5–290.0 °C.

**6-Carboxy-2-(4'-fluorophenyl)-1,3-benzothiazole (8).** To a solution of **7** (2.20 g, 0.013 mol) and *p*-fluorothiobenzamide (1.55 g, 0.010 mol) in dry *N*-methylpyrrolidone (NMP, 20 mL) was added concentrated hydrochloric acid (2 mL), and the reaction mixture was protected from light and heated (100 °C) for 8 h. After cooling to room temperature, the mixture was poured over crushed ice. The precipitate was filtered off, washed with water, and dried in a vacuum oven. The residue was purified with silica column chromatography using dichloromethane as eluent to yield 0.36 g of **8** as a yellow solid (0.0013 mol, 13%). <sup>1</sup>H NMR (DMSO-*d*<sub>6</sub>, 200 MHz):  $\delta$  7.44 (t, 2H,  $^3J = 8.8$  Hz, 3'-H 5'-H),  $\delta$  8.11 (s, 1H, 4-H),  $\delta$  8.20 (dd, 2H,  $^3J = 8.5$  Hz,  $^4J = 2.6$  Hz, 2'-H 6'-H),  $\delta$  8.32 (d, 1H,  $^4J = 1.0$  Hz, 5-H),  $\delta$  8.78 (s, 1H, 7-H). Accurate MS ES<sup>+</sup>  $m/z$  [M + H]<sup>+</sup> 274.0339 (calculated for C<sub>14</sub>H<sub>8</sub>FNO<sub>2</sub>S 274.0333). Mp: 133.7–134.2 °C.

**Production of [<sup>18</sup>F]Fluoride and Radiosynthesis of 6-Methoxy-2-(4'-[<sup>18</sup>F]fluorophenyl)-1,3-benzothiazole [<sup>18</sup>F]**3a**, 6-Hydroxy-2-(4'-[<sup>18</sup>F]fluorophenyl)-1,3-benzothiazole [<sup>18</sup>F]**3b**, and 6-Methyl-2-(4'-[<sup>18</sup>F]fluorophenyl)-1,3-benzothiazole [<sup>18</sup>F]**5**.** [<sup>18</sup>F]Fluoride was produced via a [<sup>18</sup>O(p,n)<sup>18</sup>F] reaction by irradiation of 0.5 mL of 97% enriched H<sub>2</sub><sup>18</sup>O (Rotem HYOX, <sup>18</sup> Rotem Industries, Beer

Sheva, Israel) in a niobium target using 18 MeV protons from a Cyclone 18/9 cyclotron (Ion Beam Applications, Louvain-la-Neuve, Belgium). The aqueous solution of [<sup>18</sup>F]F<sup>–</sup> was transferred to a synthesis module where [<sup>18</sup>F]F<sup>–</sup> was separated from H<sub>2</sub><sup>18</sup>O using a Sep-Pak Light Waters Accell Plus CM cartridge (Waters). [<sup>18</sup>F]F<sup>–</sup> was then eluted from the cartridge into a reaction vial with a solution containing 2.5 mg of potassium carbonate and 27.9 mg of Kryptofix 2.2.2 dissolved in 0.75 mL of water/acetonitrile (5:95 v/v). After evaporation of the solvent from the reaction vial under a stream of helium at 115 °C for 7 min, [<sup>18</sup>F]F<sup>–</sup> was further dried by azeotropic distillation of traces of water using 1 mL of anhydrous acetonitrile (115 °C, 5 min). A solution of 1.5 mg of precursor in 0.5 mL of anhydrous DMSO was added to the radioactive residue of K[<sup>18</sup>F]F<sup>–</sup> Kryptofix, and the mixture was heated at 150 °C for 20 min in a closed vial to provide the crude radiolabeled compound. For the synthesis of 6-hydroxy-2-(4'-[<sup>18</sup>F]fluorophenyl)-1,3-benzothiazole ([<sup>18</sup>F]**3b**), 0.5 mL of a mixture of methanol/concentrated HCl (2:1 v/v) was added after the radiolabeling reaction, and the mixture was heated at 125 °C for 5 min. To neutralize the reaction mixture, 1 mL of 2 M sodium acetate was added. The crude mixtures were allowed to cool to room temperature and were diluted with 0.5 mL of Tween 1% in water and applied onto a Sep-Pak Plus C18 cartridge (Waters) that was first rinsed two times with 2 mL of water/ethanol (75:25 v/v) and then eluted with 600  $\mu$ L of ethanol. After dilution with an equal volume of water, the resulting water/ethanol mixture was applied onto an XTerra Prep RP<sub>18</sub> 10 mm  $\times$  250 mm column (Waters) that was eluted with an isocratic mixture of 50% 0.05 M NH<sub>4</sub>OAc and 50% ethanol/tetrahydrofuran (75:25 v/v) at a flow rate of 3 mL/min. Radiolabeled 6-methoxy-2-(4'-[<sup>18</sup>F]fluorophenyl)-1,3-benzothiazole ([<sup>18</sup>F]**3a**) and 6-hydroxy-2-(4'-[<sup>18</sup>F]fluorophenyl)-1,3-benzothiazole ([<sup>18</sup>F]**3b**) were collected at 19 min, whereas their precursors **3e** and **3f** eluted at 24 min. Radiolabeled 6-methyl-2-(4'-[<sup>18</sup>F]fluorophenyl)-1,3-benzothiazole ([<sup>18</sup>F]**5**) was collected at 41 min, whereas the precursor **3h** eluted at 48 min. The fractions containing the isolated radioactive compound were diluted with an equal volume of water and were then applied on an activated Sep-Pak Plus C18 cartridge (Waters) that was first rinsed with water and then eluted with 1 mL of ethanol. The purity of the labeled tracers was analyzed using an XTerra RP<sub>18</sub> 5  $\mu$ m, 4.6 mm  $\times$  250 mm column (Waters) eluted with an isocratic mixture of 50% 0.05 M NH<sub>4</sub>OAc and 50% ethanol/tetrahydrofuran (75:25 v/v) at a flow rate of 1 mL/min ( $t_R$  [<sup>18</sup>F]**3a** = 20.65 min,  $t_R$  [<sup>18</sup>F]**3b** = 12.81 min, and  $t_R$  [<sup>18</sup>F]**5** = 31.37 min). Decay corrected radiochemical yields, corrected for the fraction of [<sup>18</sup>F]fluoride retained on the Sep-Pak Light Accell plus QMA anion exchange cartridge, were 24.1  $\pm$  2.3% for [<sup>18</sup>F]**3a**, 38.0  $\pm$  0.2% for [<sup>18</sup>F]**3b**, and 29.4  $\pm$  3.2% for [<sup>18</sup>F]**5**. The overall synthesis time to obtain the pure product was between 60 and 80 min. The average specific activity was found to be 116 GBq/ $\mu$ mol at end of synthesis.

**Binding Studies.** Binding studies were carried out according to a method described previously.<sup>34</sup> [<sup>125</sup>I]IMPY (6-iodo-2-(4'-dimethylamino)phenylimidazo[1,2]pyridine) with a specific activity of 81.4 TBq/mmol and greater than 95% radiochemical purity was prepared using a standard iododestannylation reaction and purified using a simplified C-4 minicolumn as described previously.<sup>14</sup> Binding assays were carried out in 12 mm  $\times$  75 mm borosilicate glass tubes. The reaction mixture contained 50  $\mu$ L of post mortem AD brain homogenate (20–50  $\mu$ g), 50  $\mu$ L of [<sup>125</sup>I]IMPY solution (0.04–0.06 nM diluted in phosphate buffered saline (PBS)), and 50  $\mu$ L of solutions of the test compound (10<sup>–5</sup>–10<sup>–10</sup> M diluted serially in PBS containing 0.1% bovine serum albumin) in a final volume of 1 mL. Nonspecific binding was defined in the presence of 600 nM nonradioactive IMPY in the same assay tubes. The mixtures were incubated at 37 °C for 2 h, and the bound and free radioactivity was separated by vacuum filtration through Whatman GF/B filters using a Brandel M-24R cell harvester (Brandel, Gaithersburg, MD) followed by two 3-mL washes with PBS at room temperature. Filters containing the bound iodine-125 labeled ligand were counted in a  $\gamma$  counter with 70% counting efficacy. Under the assay conditions, the specifically bound fraction was less than 15% of total radioactivity. The results of inhibition experiments

were subjected to nonlinear regression analysis using EBDA,<sup>35</sup> from which  $K_i$  values were calculated.

**Partition Coefficient Determination.** The lipophilicity of the RP-HPLC isolated <sup>18</sup>F complexes was determined using a modification of the method described by Yamauchi and co-workers.<sup>36</sup> A 25  $\mu$ L aliquot of the RP-HPLC isolated solution of the <sup>18</sup>F-labeled compound was added to a tube containing 2 mL of 1-octanol and 2 mL of 0.025 M phosphate buffer, pH 7.4 ( $n = 6$ ). The test tube was vortexed at room temperature for 3 min followed by centrifugation at 3000 rpm (1837g) for 10 min (Eppendorf centrifuge 5810, Eppendorf, Westbury). Aliquots of 61 and 500  $\mu$ L were drawn from the 1-octanol and buffer phases, respectively, taking care to avoid cross-contamination between the two phases and weighed. The radioactivity in the aliquots was counted using an automatic  $\gamma$  counter. After correction for the density and the mass difference between the two phases, the partition coefficient ( $P$ ) was calculated using the following equation:

$$P = \frac{(\text{cpm})/(\text{mL of octanol})}{(\text{cpm})/(\text{mL of buffer})}$$

with cpm = counts per minute.

**Biodistribution in Normal Mice.** A solution of [<sup>18</sup>F]3a, [<sup>18</sup>F]3b, and [<sup>18</sup>F]5 obtained after RP-HPLC purification was diluted using 0.9% NaCl in water for injection to a concentration of 3.7 MBq/mL. The concentration of ethanol did not exceed 10%, and the concentration of THF did not exceed 0.02%, as determined by gas chromatography. The biodistribution was studied in male NMRI mice (body mass of 30–40 g). An aliquot of 0.1 mL of the diluted tracer solution was injected into the mice via a tail vein, after intraperitoneal injection of 0.1 mL Hypnorm (fentanyl citrate 63  $\mu$ g/mL and fluanisone 2 mg/mL). The mice were sacrificed by decapitation at 2 or 60 min p.i. Blood was collected in a tared tube and weighed. All organs and other body parts were dissected and weighed, and their radioactivity was counted in a  $\gamma$  counter. Results were corrected for background radioactivity and are expressed as percentage of the injected dose (% ID) or as percentage of the injected dose per gram of tissue (% ID/g). For calculation of total radioactivity in blood, blood mass was assumed to be 7% of the total body mass.

**$\mu$ PET Study in a Normal Rat.** A rat (300 g, male Wistar rat) was anesthetized with isoflurane (1.5–2.5%) in oxygen at a flow rate of 1–2 L/min and was injected with 1.41 MBq [<sup>18</sup>F]3a, 9.69 MBq [<sup>18</sup>F]3b, or 6.18 MBq [<sup>18</sup>F]5 via a tail vein with a time interval of 5 days between each tracer injection. The rat was breathing spontaneously throughout the entire experiment. Dynamic  $\mu$ PET images were acquired for 120 min (4  $\times$  15 s, 4  $\times$  60 s, 5  $\times$  180 s, 8  $\times$  300 s, 6  $\times$  600 s), and reconstruction was done using filtered back-projection with a RAMP 0.5 filter. Data were analyzed using PMOD2.7. Volumes of interest (VOIs) were defined on the summed images, and time–activity curves (TACs) were drawn. The same rat was injected 2 weeks earlier with 35.3 MBq [<sup>11</sup>C]PIB in a separate study where dynamic  $\mu$ PET images were acquired for 90 min (4  $\times$  15 s, 4  $\times$  60 s, 5  $\times$  180 s, 14  $\times$  300 s).

**Plasma Radiometabolite Analysis after Injection of [<sup>18</sup>F]5 in Normal Mice.** After intravenous injection of 5.55–7.40 MBq [<sup>18</sup>F]5 via a tail vein, normal male NMRI mice were sacrificed by decapitation at 2, 10, 30, or 60 min p.i. ( $n = 3$  at each time point). Blood was collected into a BD vacutainer (containing 7.2 mg of K<sub>2</sub>EDTA; BD, Franklin Lakes). The samples were centrifuged at 3000 rpm (1837g) for 5 min at 4  $^{\circ}$ C (Eppendorf centrifuge 5810) to separate plasma. The supernatant plasma sample was mixed with 25  $\mu$ L of solution containing the authentic nonradioactive compound 5 (1 mg/mL acetonitrile), and the mixture was injected onto an Oasis HLB column (25  $\mu$ m, 4.6 mm  $\times$  20 mm, Waters) that was preconditioned by successive washings with acetonitrile and water. The proteins of the biological matrix were washed from the Oasis column with 10 mL of water (fraction 1). The outlet of the Oasis column was then connected to an XTerra RP C18 column (5  $\mu$ m, 4.6 mm  $\times$  250 mm), and both columns in series were then eluted using 0.05 M sodium acetate (pH 5.5)/acetonitrile (40:60 v/v) as the mobile phase at a flow rate of 1.5 mL/min. After passing through

an in-line UV detector (234 nm), the HPLC eluate was collected in 1.5 mL fractions and their radioactivity and the activity in fraction 1 were measured using a  $\gamma$  counter.

**Brain Radiometabolite Analysis after Injection of [<sup>18</sup>F]5 in Normal Mice.** After intravenous injection of 5.55 MBq of [<sup>18</sup>F]5 via a tail vein, normal male NMRI mice ( $n = 3$ ) were sacrificed by decapitation at 2 or 60 min p.i. The brain was removed, and 100  $\mu$ L of solution containing the authentic nonradioactive 5 (1 mg/mL acetonitrile), 2 mL of acetonitrile, and 2 mL of water were added, and the mixture was homogenized. After centrifugation at 3000 rpm (1837g) for 5 min at 4  $^{\circ}$ C (Eppendorf centrifuge 5810), 1 mL of supernatant was filtered (0.22  $\mu$ m pore size/10 mm diameter), and the filtrate was analyzed on an XTerra RP C18 column (5  $\mu$ m, 4.6 mm  $\times$  250 mm) eluted with a mixture of 0.05 M sodium acetate (pH 5.5)/acetonitrile (40:60 v/v) at a flow rate of 1.5 mL/min. After passing through an in-line UV detector (234 nm), the HPLC eluate was collected in 1.5 mL fractions and their radioactivity was measured using a  $\gamma$  counter.

**Brain Radiometabolite Analysis after Injection of [<sup>18</sup>F]5 in Normal Rat.** After intravenous injection of 7.4 MBq [<sup>18</sup>F]5 via a tail vein, a normal male Wistar rat was sacrificed with an overdose Nembutal (pentobarbital) at 2 min p.i. After the heart and blood vessels were rinsed with saline, the brain was removed. The 1 mL of a solution containing the authentic nonradioactive compound 5 (1 mg/mL acetonitrile), 2 mL of acetonitrile, and 2 mL of water were added and the mixture was homogenized. After centrifugation at 3000 rpm (1837g) for 5 min at 4  $^{\circ}$ C (Eppendorf centrifuge 5810), 1 mL of supernatant was filtered (0.22  $\mu$ m/10 mm) and the filtrate was analyzed on an XTerra RP C18 column (5  $\mu$ m, 4.6 mm  $\times$  250 mm) eluted with a mixture of 0.05 M sodium acetate (pH 5.5)/acetonitrile (40:60 v/v) at a flow rate of 1.5 mL/min. After passing through an in-line UV detector (234 nm), the HPLC eluate was collected in 1.5 mL fractions and their radioactivity was measured using a  $\gamma$  counter.

**Supporting Information Available:** Additional <sup>1</sup>H NMR, MS, and HPLC analysis data for the synthesized final products. This material is available free of charge via the Internet at <http://pubs.acs.org>.

## References

- (1) Selkoe, D. J. Alzheimer's disease: genes, proteins, and therapy. *Phys. Rev.* **2001**, *81*, 741–766.
- (2) Alzheimer, A. Uber eine eigenartige erkrankung der hirnrinde. *Allg. Z. Psychiatr.* **1907**, *64*, 146–148.
- (3) Hardy, J.; Selkoe, D. J. The amyloid hypothesis of Alzheimer's disease: progress and problems on road to therapeutics. *Science* **2002**, *297*, 353–356.
- (4) Vallet, P. G.; Guntern, R.; Hof, P. R.; Golaz, J.; Delacourte, A.; Robakis, N. K.; Bouras, C. A comparative study of histological and immunohistochemical methods for neurofibrillary tangles and senile plaques in Alzheimer's disease. *Acta Neuropathol.* **1992**, *83*, 170–178.
- (5) Ono, M.; Wilson, A.; Nobrega, J.; Westaway, D.; Verhoeff, P.; Zhuang, Z. P.; Kung, M. P.; Kung, H. F. <sup>11</sup>C-labeled stilbene derivatives as A $\beta$ -aggregate-specific PET imaging agents for Alzheimer's disease. *Nucl. Med. Biol.* **2003**, *30*, 565–571.
- (6) Verhoeff, N.; Wilson, A.; Takeshita, S.; Trop, L.; Hussey, D.; Singh, K.; Kung, H. F.; Kung, M. P.; Houle, S. In-vivo imaging of Alzheimer's disease  $\beta$ -amyloid with [<sup>11</sup>C]SB-13 PET. *Am. J. Geriatr. Psychiatr.* **2004**, *12*, 584–595.
- (7) Agdeppa, E.; Kepe, V.; Liu, J.; Flores-Torres, M.; Satyamurthy, N.; Petric, A.; Cole, G.; Small, G.; Huang, S. C.; Barrio, J. Binding characteristics of radiofluorinated 6-dialkylamino-2-naphthylethylidene derivatives as positron emission tomography imaging probes for  $\beta$ -amyloid plaques in Alzheimer's disease. *J. Neurosci.* **2001**, *21*, 1–5.
- (8) Small, G.; Kepe, V.; Ercoli, L.; Siddarth, P.; Bookheimer, S.; Miller, K.; Lavretsky, H.; Burggren, A.; Cole, G.; Vinters, H.; Thompson, P.; Huang, S. C.; Satyamurthy, N.; Phelps, M.; Barrio, J. PET of brain amyloid and tau in mild cognitive impairment. *N. Engl. J. Med.* **2006**, *355*, 2652–2663.
- (9) Zhuang, Z. P.; Klunk, W. E.; Wang, J.; Huang, G. F.; Debnath, M. L.; Holt, D. P.; Mathis, C. A. Radioiodinated styrylbenzenes and thioflavins as probes for amyloid aggregates. *J. Med. Chem.* **2001**, *44*, 1905–1914.

- (10) Klunk, W. E.; Wang, Y.; Huang, G.; Debnath, M. L.; Holt, D. P.; Mathis, C. A. Uncharged thioflavin-T derivatives bind to amyloid-beta protein with high affinity and readily enter the brain. *Life Sci.* **2001**, *69*, 1471–1484.
- (11) Klunk, W. E.; Engler, H.; Nordberg, A.; Wang, Y.; Blomqvist, G.; Holt, D.; Bergström, M.; Savitcheva, I.; Huang, G.; Estrada, S.; Ausén, B.; Debnath, M.; Barletta, J.; Price, J. C.; Sandell, J.; Lopresti, B.; Wall, A.; Koivisto, P.; Antoni, G.; Mathis, C.; Langström, B. Imaging brain amyloid in Alzheimer's disease with Pittsburgh compound-B. *Ann. Neurol.* **2004**, *55*, 306–319.
- (12) Archer, H.; Edison, P.; Brooks, D.; Barnes, J.; Frost, C.; Yeatman, T.; Fox, N.; Rossor, M. Amyloid load and cerebral atrophy in Alzheimer's disease: an <sup>11</sup>C-PIB positron emission tomography study. *Ann. Neurol.* **2006**, *60*, 145–147.
- (13) Zhuang, Z. P.; Kung, M. P.; Hou, C.; Plossel, K.; Skovronsky, D.; Gur, T. L.; Trojanowski, J. Q.; Lee, V.; Kung, H. F. IBOX(2-(4'-dimethylaminophenyl)-6-iodobenzoxazole): a ligand for imaging amyloid plaques in the brain. *Nucl. Med. Biol.* **2001**, *28*, 887–894.
- (14) Zhuang, Z. P.; Kung, M. P.; Wilson, A.; Lee, C. W.; Plössl, K.; Hou, C.; Holtzman, D.; Kung, H. F. Structure–activity relationship of imidazo[1,2-*a*]pyridines as ligands for detecting  $\beta$ -amyloid plaques in the brain. *J. Med. Chem.* **2003**, *46*, 237–243.
- (15) Suemoto, T.; Okamura, N.; Shiomitsu, T.; Suzuki, M.; Shimadzu, H.; Akatsu, H.; Yamamoto, T.; Kudo, Y.; Sawada, T. In vivo labeling of amyloid with BF-108. *Neurosci. Res.* **2004**, *48*, 65–74.
- (16) Zhang, W.; Oya, S.; Kung, M. P.; Hou, C.; Maier, D.; Kung, H. F. F-18 polyethyleneglycol stilbenes as PET imaging agents targeting A $\beta$  aggregates in the brain. *Nucl. Med. Biol.* **2005**, *32*, 799–809.
- (17) Chang, Y.; Jeong, J.; Lee, Y. S.; Kim, H.; Rai, G.; Kim, Y.; Lee, D.; Chung, J. K.; Lee, M. Synthesis and evaluation of benzothiophene derivatives as ligands for imaging  $\beta$ -amyloid plaques in Alzheimer's disease. *Nucl. Med. Biol.* **2006**, *33*, 811–820.
- (18) Zhuang, Z. P.; Kung, M. P.; Kung, H. F. Synthesis of biphenyltrienes as probes for  $\beta$ -amyloid plaques. *J. Med. Chem.* **2006**, *49*, 2841–2844.
- (19) Sato, K.; Higuchi, M.; Iwata, N.; Saido, T.; Sasamoto, K. Fluoro-substituted and <sup>13</sup>C-labeled styrylbenzene derivatives for detecting brain amyloid plaques. *Eur. J. Med. Chem.* **2004**, *39*, 573–578.
- (20) Zhuang, W.; Kung, M. P.; Oya, S.; Hou, C.; Kung, H. F. <sup>18</sup>F-labeled styrylpyridines as PET agents for amyloid plaque imaging. *Nucl. Med. Biol.* **2007**, *34*, 89–97.
- (21) Ryu, E.; Choe, Y.; Lee, K. H.; Choi, Y.; Kim, B. T. Curcumin and dehydrozingerone derivatives: synthesis, radiolabelling, and evaluation for  $\beta$ -amyloid plaque imaging. *J. Med. Chem.* **2006**, *49*, 6111–6119.
- (22) Shi, D.; Bradshaw, T.; Wrigley, S.; McCall, C.; Lelieveld, P.; Fichtner, I.; Stevens, M. Antitumor benzothiazoles. 3. Synthesis of 2-(4-aminophenyl)benzothiazoles and evaluation of their activities against breast cancer cell lines in vitro and in vivo. *J. Med. Chem.* **1996**, *39*, 3375–3384.
- (23) Kashiyama, E.; Hutchinson, I.; Chua, M.-S.; Stinson, S.; Phillips, L.; Kaur, G.; Sausville, E.; Bradshaw, T.; Westwell, A.; Stevens, M. Antitumor benzothiazoles. 8. Synthesis, metabolic formation, and biological properties of the C- and N-oxidation products of antitumor 2-(4-aminophenyl)benzothiazoles. *J. Med. Chem.* **1999**, *42*, 4172–4184.
- (24) Hutchinson, I.; Chua, M.-S.; Browne, H.; Trapani, V.; Bradshaw, T.; Westwell, A.; Stevens, M. Antitumor benzothiazoles. 14. Synthesis and in vitro biological properties of fluorinated 2-(4-aminophenyl)benzothiazoles. *J. Med. Chem.* **2001**, *44*, 1446–1455.
- (25) Cava, M.; Levinson, M. Thionation reactions of Lawesson's reagents. *Tetrahedron* **1985**, *41*, 5061–5087.
- (26) von Manfred, S.; Siegfried, J.; Manfred, H. Synthese und reaktionsverhalten 2'-substituierter isoflavone. *Helv. Chim. Acta* **1992**, *75*, 457–470.
- (27) Lin, A.; Kasina, S. Synthesis of 3-substituted 7-(3,3-dimethyl-1-triazeno)-10-methylphenothiazines as potential antitumor agents. *J. Heterocycl. Chem.* **1981**, *18*, 759–761.
- (28) Mashraqui, S.; Kumar, S.; Trần Huu Dầu, E. Synthesis, molecular structure and optical spectral studies of *syn*-dithia benzothiazolophane and *anti*-bis-lactone benzothiazolophane. *J. Mol. Struct.* **2004**, *697*, 221–230.
- (29) Lang, R.; Williams, C.; Garson, M. An improved preparation of 4-amino-3-mercaptobenzoic acid. *Org. Prep. Proced. Int.* **2003**, *35*, 520–524.
- (30) Dishino, D.; Welch, M.; Kilbourn, M.; Raichle, M. Relationship between lipophilicity and brain extraction of C-11-labeled radiopharmaceuticals. *J. Nucl. Med.* **1983**, *24*, 1030–1038.
- (31) Chitneni, S. K.; Serdons, K.; Evens, N.; Fonge, H.; Celen, S.; Deroose, C. M.; Debyser, Z.; Mortelmans, L.; Verbruggen, A. M.; Bormans, G. M. Efficient purification and metabolite analysis of radiotracers using high-performance liquid chromatography and on-line solid-phase extraction. *J. Chromatogr., A* **2008**, *1189*, 323–331.
- (32) Mathis, C. A.; Holt, D.; Wang, Y.; Huang, G.-F.; Debnath, M.; Shao, L.; Klunk, W. E. Species-dependent formation and identification of the brain metabolites of the amyloid imaging agent [<sup>11</sup>C]PIB. *Neurobiol. Aging* **2004**, *25* (S2), 277.
- (33) Solbach, C.; Uebele, M.; Reischl, G.; Machulla, H.-J. Efficient radiosynthesis of carbon-11 labelled uncharged thioflavin T derivatives using [<sup>11</sup>C]methyl triflate for  $\beta$ -amyloid imaging in Alzheimer's disease with PET. *Appl. Radiat. Isot.* **2005**, *62*, 591–595.
- (34) Kung, M. P.; Hou, C.; Zhuang, Z. P.; Skovronsky, D.; Kung, H. F. Binding of two potential imaging agents targeting amyloid plaques in postmortem brain tissues of patients with Alzheimer's disease. *Brain Res.* **2004**, *1025*, 89–105.
- (35) Munson, P. J.; Rodbard, D. Ligand: a versatile computerized approach for characterisation of ligand-binding systems. *Anal. Biochem.* **1980**, *107*, 220–239.
- (36) Yamauchi, H.; Takahashi, J.; Seri, S.; Kawashima, H.; Koike, H.; Kato-Azuma, M. In *Technetium and Rhenium in Chemistry and Nuclear Medicine*; Nicolini, M., Bandoli, G., Mazzi, U., Eds.; Cortina International: Verona, Italy, 1989; pp 475–502; Vol. 3.

JM8013376